Cytogenetic characterisation and proteomic profiling of the Imatinib-resistant cell line KCL22-R

JULIA ROSENHAHN[1*], ANJA WEISE[3*], SUSANNE MICHEL[4], KATRIN HENNIG[2], ISABELL HARTMANN[2], JANA SCHIEFNER[2], KATRIN SCHUBERT[1], THOMAS LIEHR[3], FERDINAND VON EGGELING[1] and IVAN F. LONCAREVIC[2]

[1]Core Unit Chip Application, Institute of Human Genetics and Anthropology, [2]Tumor Genetics, Institute of Human Genetics and Anthropology, [3]Molecular Cytogenetics, Institute of Human Genetics and Anthropology, [4]Institute of Human Genetics and Anthropology, Medical Faculty at the Friedrich Schiller University Jena, Germany

Received February 5, 2007; Accepted March 26, 2007

Abstract. Approximately 30% of chronic myeloid leukemia patients show initially no response to Imatinib, a potent inhibitor of BCR-ABL. This intrinsic resistance may be due to BCR-ABL-independent cell growth. Here we analysed the cytogenetic anomalies and the proteomic profiling in KCL22-S and KCL22-R, two Imatinib-sensitive and -resistant derivative cell lines of KCL22. A tetrasomy 8 and a non-reciprocal translocation +der(6)t(6;13)(p11.1;q12) were found only in KCL22-R as new evolved anomalies. Chromosome der(6)t(6;13) showed four variants differing in the chromatin content of 13q14-13qter including the retinoblastoma gene. Due to these sub-clones, approximately 65-79% of the Imatinib-treated KCL22-R cells showed a disomy and 21-35% a monosomy for 13q14. Imatinib removal reduced the main clone to approximately 20% in the benefit of the monosomic sub-clones. This was accompanied by an increased apoptosis rate and was revertible by Imatinib re-treatment. This effect may be connected with genes located in 13q14-qter. Proteomic profiling of the cell lines performed with ProteinChip technology (SELDI) revealed several differentially expressed proteins (n=45). In summary, we demonstrate here the complex changes on the cytogenetic and proteomic level which could be caused by Imatinib and the resistance resulting from it.

Introduction

Imatinib (STI571, Gleevec®) is a relatively new type of anti-cancer medication that can effectively block the proliferation in chronic myeloid leukemia (CML). It acts by inhibiting the tyrosine kinase BCR-ABL, a characteristic feature of CML that results predominantly from a reciprocal chromosomal translocation t(9;22)(q34;q11) (1,2). The BCR-ABL gene encodes for a constitutively active tyrosine kinase which is involved in a multitude of signalling and survival pathways that result in enhanced proliferation, decreased apoptosis and reduced adhesion of tumor cells (3-5).

Although Imatinib is a very potent drug for targeting patients in the chronic phase of the disease, the response rates decrease during disease progression (6). This type of primary Imatinib resistance strictly differs from the drug-induced acquired resistance. The latter is caused either by mutations in the ATP-binding site of BCR-ABL or by its overexpression (7-9). Patients showing acquired resistance respond initially to Imatinib but relapse within 12 months. Primary resistance to Imatinib, on the other hand, is observed in 20-30% of newly diagnosed patients (5) and in 22-50% of patients in accelerated or blastic phase (10). It is characterised by a proliferation of tumor cells independent of BCR-ABL activity. However, what substitutes BCR-ABL function in those Imatinib-resistant cells is not well understood.

Surprisingly, the role of chromosomal changes has not been investigated in the context of primary Imatinib resistance to date albeit chromosomal changes and clonal evolution are clearly associated with disease progression in CML (11). Approximately 71% of patients with CML in blast crisis show chromosomal changes in addition to t(9;22). The most frequent secondary aberrations are gains of the Philadelphia chromosome, chromosomes 1, 2, 6, 7, 8 16, 17, 19 or 21 as well as a loss of chromosomes 3, 5, 7, 17 or 19 (12). Chromosomal changes have also been shown to develop from Imatinib therapy. These aberrations affect neither additional chromosomes nor do they result in a new Imatinib-resistant clone (13). So far no relationship between additional chromosomal changes and Imatinib resistance could be conclusively deduced.

ProteinChip technology (SELDI; surface-enhanced laser desorption/ionization) is a proteomic high-throughput technique that uses chromatographic surfaces able to retain proteins depending on their physico-chemical properties followed by direct analysis via time of flight mass spectrometry (TOF-MS)

Correspondence to: Dr Ferdinand von Eggeling, Core Unit Chip Application, Institute of Human Genetics and Anthropology, FSU Jena, Germany
E-mail: ferdinand.voneggeling@mti.uni-jena.de

*Contributed equally

Key words: chronic myeloid leukemia, BCR-ABL, Imatinib, initial resistance, karyotype evolution, SELDI

(14). A multitude of studies using the ProteinChip technology were carried out for protein profiling of cells and body fluids (15-22).

In the present study we used cytogenetic analysis to characterise the Imatinib-sensitive and -resistant CML cell lines KCL22-S and -R to discriminate for numerical and structural chromosome aberrations and proteomic profiling to find differentially expressed proteins. Accordingly, we have identified characteristic chromosomal aberrations in the resistant cells and 45 differentially expressed proteins. These results provide *in vitro* evidence that Imatinib has an influence on specific chromosome aberrations and thereby causes several alterations in the proteome which may lead conclusively to resistance.

Materials and methods

Cell lines and cell proliferation/apoptosis analysis. The Imatinib-resistant cell line KCL22-R and its sensitive counterpart KCL22-S were established by Mahon and co-workers (23) to analyse primary Imatinib resistance *in vitro*. The parental cell line KCL22 is initially resistant to Imatinib (23) and consists of sensitive and resistant subpopulations, which can be isolated from the original cell line using methylcellulose. The KCL22-R cells employed in this study neither bear mutations in the ATP-binding site of BCR-ABL nor show BCR-ABL overexpression (23). Therefore, they represent an adequate *in vitro* system to analyse Imatinib resistance which is based on a BCR-ABL-independent growth capacity. Cells were cultured in RPMI (Pan Biotech GmbH) with 10% FCS (Biochrom) in a 5% CO_2 atmosphere at 37˚C and were passaged twice weekly. The Imatinib-resistant cell line KCL22-R1$^+$ was grown in the presence of 1 μM Imatinib. The tyrosine kinase inhibitor Imatinib, kindly provided by Andrea Uecker (Molecular Cell Biology department, FSU Jena), was prepared in sterile DMSO as a 10 mM stock solution and diluted to a working concentration of 100 μM with sterile PBS. We established a non-treated resistant clone from KCL22-R1$^+$ by growing cells for three to six months without Imatinib (KCL22-R1$^-$). These cells were used to analyse changes associated with Imatinib therapy.

For proliferation assays, cells were seeded at a concentration of 1x10^5 cells per ml. Counting of cells was performed every 24 h using a Neubauer counting grid. Cells were stained with 0.5% Trypan Blue solution and vital cells were counted after 5 min at 37˚C. The growth rate was defined as the average of the percentage increase of cell number over the five days of culturing.

Apoptosis was examined with the Apo-ONE® homogeneous caspase-3/7 assay kit (Promega) after 20 h of treatment with Imatinib or vehicle. Cells were harvested by centrifugation and resuspended in 100 μl PBS. The suspension (20 μl) was mixed with 20 μl Apo-ONE Assay solution and incubated for 2-4 h in the dark. Fluorescence was measured with a SpectraMAX Gemini spectrometer (Molecular Devices).

Cytogenetics and FISH. Chromosome preparations and GTG-banding analysis were performed according to standard protocols (24). Analysis of approximately 10 metaphases was carried out using an Axioplan 2 microscope (Zeiss, Germany).

Multiplex-FISH (M-FISH) was performed to confirm GTG-results as described by Weise and co-workers (25). Ten metaphase images per cell line were captured on a fluorescence microscope (Axioplan 2, Zeiss, Germany) with a PCO VC45 CCD camera (PCO, Kehl, Germany) and suitable filter combinations (DAPI/FITC/Spectrum Orange/Texas Red/Cyanine 5/Cyanine 5.5) using ISIS3-software (MetaSystems, Altlussheim, Germany). 24-Color-FISH using all 24 human whole chromosome painting probes was applied to identify interchromosomal rearrangements (25).

To quantify relevant M-FISH data, interphase nuclei were hybridised with the centromere probe cep 6 (Spectrum Green), cep8 (Spectrum Green or Spectrum Aqua) and a retinoblastoma (Rb) gene (13q14.3) locus specific probe LSI 13S319 (Spectrum Orange) (Abbott) as previously described (24). Signals of 200-250 interphase nuclei were analysed. The 'cut-off' for trisomy/tetrasomy 8 and monosomy 13q14 was 4% and 8%, respectively according to lab standards based on the analysis of 200-250 cells. BCR-ABL breakpoint was confirmed using LSI Dual Color Dual Fusion probe (Abbott) and by PCR using oligonucleotides as described (26).

High resolution multi-color banding (MCB) was performed to analyse the breakpoints in chromosome der(6)t(6;13)(q11.1;q12). Overlapping microdissected labelled probe sets were hybridised on metaphase spreads as described previously (27).

ProteinChip Array analysis. Cells were lysed with 9.5 M urea, 2% CHAPS, 1% DTT for 15 min at RT and centrifuged at 12000 x g for 15 min. Protein concentration of supernatants was measured by the Bradford method. Equal amounts of protein (30-50 mg/ml) in a total volume of 50-100 μl lysate were applied to the fractionation using QHyperD columns (Ciphergen) according to the manufacturer's guidelines. Whole cell lysates and fractionated samples were analyzed on IMAC Cu(II) protein arrays (Ciphergen Biosystems Inc, Fremont, CA) as described elsewhere (28). Mass analysis was performed in a ProteinChip Reader (series 4000, Ciphergen Biosystems Inc) according to an automated data collection protocol. After normalization based on total ion current and calibration of data, peaks with a signal-to-noise ratio of 10 were combined as clusters, using the CiphergenExpress 3.0 program (Ciphergen Biosystems). The p values were calculated by nonparametric Mann-Whitney U test (two-way comparisons), using the CiphergenExpress 3.0 program. Protein peaks with p values <0.05 were considered significantly deregulated (up-regulated or down-regulated) in lysates of KCL22-S and -R. Up to ten biological replicates were analysed using the described procedure.

Results

The effect of Imatinib on cell growth and apoptosis in KCL22-S and KCL22-R. Cell proliferation was significantly reduced in the presence of 1 μM Imatinib in both, the sensitive cell line KCL22-S and the parental cell line KCL22-P. In contrast, the resistant cell line KCL22-R exhibited an elevated growth rate in the presence of Imatinib (data not shown).

Apoptosis in KCL22-S was significantly increased (47%) after treatment with 1 μM Imatinib for one day (Fig. 1). In contrast, Imatinib caused no significant effect on the apoptosis

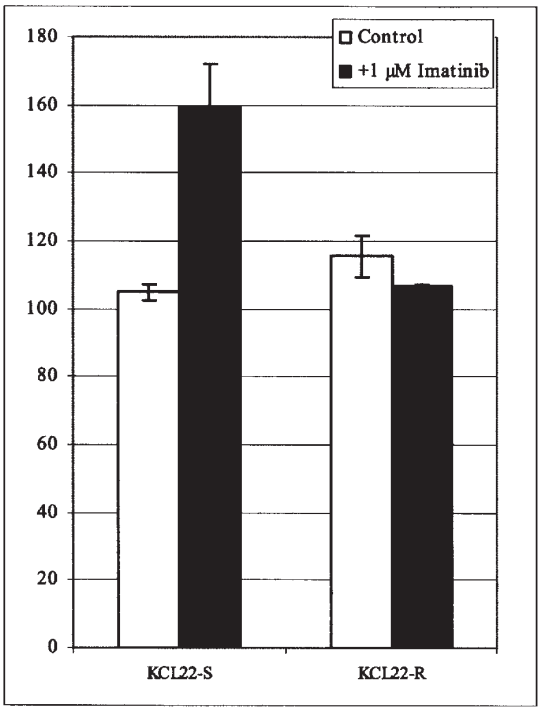

Figure 1. Apoptotic rates of KCL22-R and KCL22-S cell lines exposed to Imatinib. Caspase 3/7 activity values after 20 h in 1 μM Imatinib (+1 μM) and the controls without Imatinib. KCL22-S, Imatinib-sensitive cell line; KCL22-R$^+$, Imatinib-resistant cell line (continuously treated with Imatinib).

rate in KCL22-R. Contrarily, Imatinib even decreases caspase activity by approximately 8% in KCL22-R.

Karyotype analysis by GTG-banding and M-FISH. Ten metaphases of individual clones of each, the sensitive (KCL22-S1, KCL22-S2), the resistant (KCL22-R1$^+$ and KCL22-R2$^+$), the parental KCL22-P, and the Imatinib-deprived resistant KCL22-R1$^-$ cell lines, were analysed by GTG-banding and M-FISH. The composite karyotype of the parental cell line KCL22-P was 47~50,X,del(X)(p),+der(1)t(1;10)(p13;?), +6,+8x2,der(9)t(9;22)(q34;q11),der(17)t(17;19),i(21)(11.1), der(22)t(9;22)(q34;q11)x2[cp10]. These aberrations are in line with previously published data (29). However, we were able to obtain a more detailed characterization of these aberrations due to FISH analysis. The breakpoint in chromosome 1 was allocated to p13 and the described loss of chromosome X was restricted to Xp. KCL22-S and -R showed almost all of these aberrations (Fig. 2A and B). However, KCL22-S and KCL22-R showed an additional translocation t(8;21)(p21?;?) that was not present in the parental cell line. A non-reciprocal translocation +der(6)t(6;13)(p11.1;q12) was exclusively found in KCL22-R. The extent of the translocated material of chromosome 13 was different in individual metaphases resulting in smaller or larger chromosomes der(6)t(6;13) The sensitive cells showed also a gain of chromosome 6 but without t(6;13). A loss of one chromosome 13 was an additional characteristic feature of one KCL22-R clone.

Variants of chromosome der(6)t(6;13) in KCL22-R. Multicolor banding (MCB) was performed to map the breakpoints of the translocation t(6;13)(p11.1;q12) in KCL22-R in more detail.

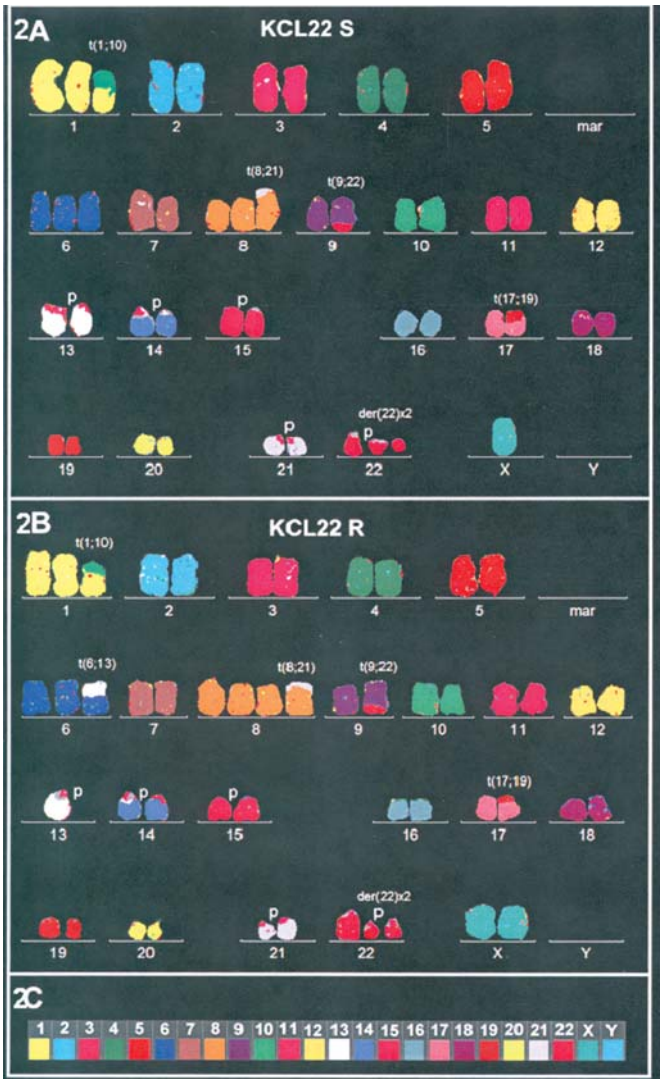

Figure 2. Molecular cytogenetic characteristics of KCL22-R and KCL22-S. Representative karyogram after 24-color-FISH of KCL22-S (A), KCL22-R (B) and the list of pseudo-colors for each individual chromosome (C). The composite karyotype of KCL22-S is 48~51,X,X,+der(1)t(1;10)(p13;?), +6,+der(8)t(8;21)(p21;q?),der(9)t(9;22)(q34;q11),der(17)t(17;19),-22, +der(22)t(9;22)(q34;q11)x2[cp10]. The composite karyotype of KCL22-R is 48~51,X,X,+der(1)t(1;10)(p13;?),+der(6)t(6;13)(p11.1;q12),+8, +der(8)t(8;21)(p21;q?),der(9)t(9;22)(q34;q11),-13,der(17)t(17;19),22, +der(22)t(9;22)(q34;q11)x2[cp8]/49~50,XX,idem,der(6)t(6;13)(p11.1;q12), +der(6)t(3;13;6)(?;p12;p11.1)[cp2].

The breakpoints in t(6;13) were assigned to 6p11.1 and 13q12 (Fig. 3). However, the portions of the translocated material of 13q varied in individual clones extending from 13q12 to different distal positions (Fig. 4). Approximately 25% of the metaphases showed a derivative chromosome 6 with a complex translocation t(3;13;6)(?;p12;p11.1) while the breakpoints on chromosomes 6 and 13 were identical to those in der(6)t(6;13). Taken together translocation t(6;13) resulted in a loss of trisomy for 6p10_pter, a monosomy for 13q10_q11, and in sub-clones with variable portions of 13q12_qter.

Subclones of KCL22-S and KCL22-R. After counting 200-250 nuclei by interphase FISH several combinations of numerical aberrations of chromosomes 8 and 13 became evident in all examined cell lines. A trisomy 8 was found in 72% of KCL22-S

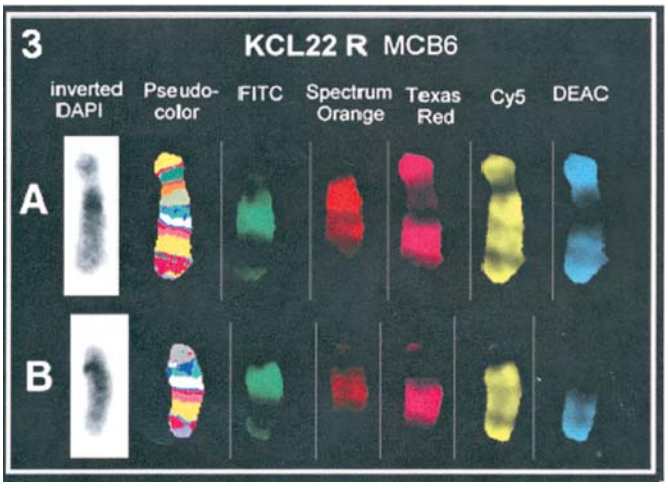

Figure 3. Multi-color banding (MCB) analysis for chromosome 6 refining the breakpoints in chromosome der(6)t(6;13). From left to right: inverted DAPI; pseudo-color image; fluorescence channels, FITC, Spectrum Orange, Texas Red, Cy5 and DEAC. A normal chromosome 6 (A) and chromosome der(6)t(6;13) (B). The breakpoint was mapped to 6p11.1.

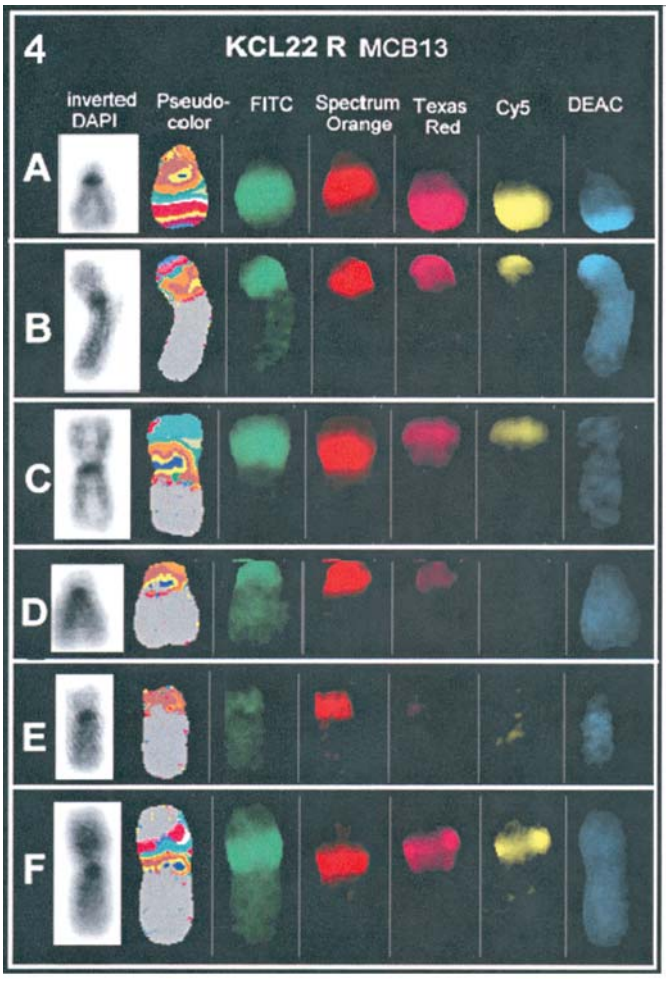

Figure 4. MCB of chromosome 13 refining the breakpoints in chromosome der(6)t(6;13). From left to right: inverted DAPI; pseudo-color image; fluorescence channels, FITC, Spectrum Orange, Texas Red, Cy5 and DEAC. A normal chromosome 13 (A) and chromosome der(6)t(6;13) (B-F). The breakpoint was mapped to 13q12. Five sub-clones with varying chromatin content from 13q14_qter: (B) der(6)t(6;13)(6qter_6p11.1::13q12_13qter), (C) der(6)t(6;13)(6qter_6p11.1::13q12_13q22), (D) der(6)t(6;13)(6qter_6p11.1::13q12_13q14), (E) der(6)t(6;13)(6qter_6p11.1::13q12_13q13) and (F) der(6)t(3;13;6)(6qter_6p11.1::13q12_13q14::3?).

and in 18% of KCL22-R cells. In contrast, the predominant subpopulation with a share of 80% showed a tetrasomy 8 in KCL22-R which occurred in <5% of KCL22-S cells. Interphase FISH employing a locus specific probe for 13q14 showed a normal FISH signal pattern for the KCL22-S cells. The KCL22-R cell line exhibited a monosomy for 13q14 in 22% and a disomy in 78% as detected in interphase FISH analysis (Fig. 6). This cell population is constituted by one or two sub-clones (sub-clone E and probably also D, see Fig. 4) lacking 13q14_qter in chromosome der(6)t(6;13)(p11.1;q12). This was confirmed by FISH on metaphase spreads providing the two types of derivative chromosome der(6) (Fig. 5).

Influence of Imatinib treatment on the size of sub-clone with monosomy 13q14. We observed an increased cell growth in KCL22-R with Imatinib compared to without. Therefore we

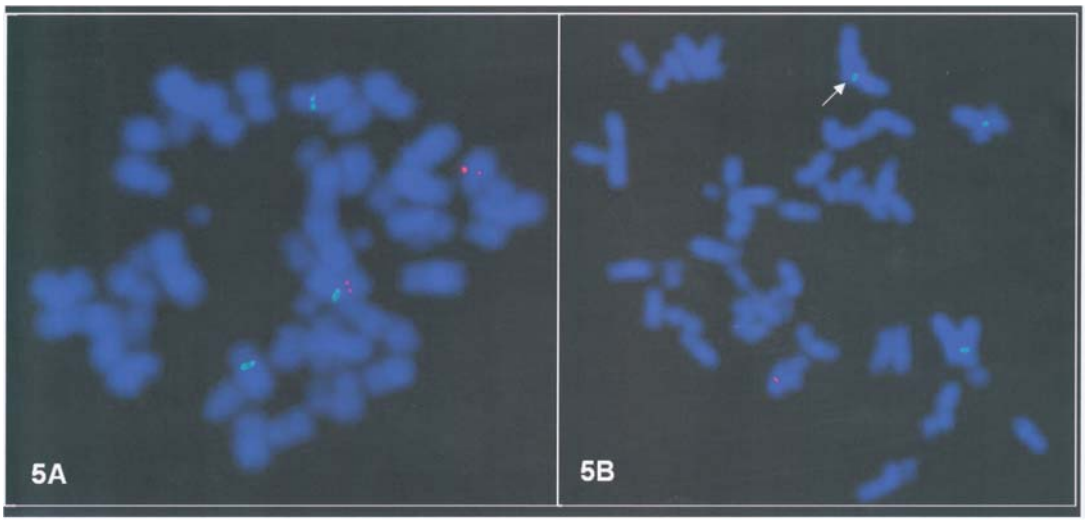

Figure 5. Representative metaphase of the prominent sub-clone in Imatinib-treated KCL22-R$^+$ (A) and Imatinib-deprived KCL22-R$^-$ (B). FISH pattern with centromer probes for chromosome 6 (Spectrum Green) and LSI 13 (Spectrum Orange) demonstrating a disomy for 13q14 (A) and a monosomy for 13q14 (B) resulting from a loss of the target sequence in chromosome der(6)t(6;13)(p11.1;q12) (arrow).

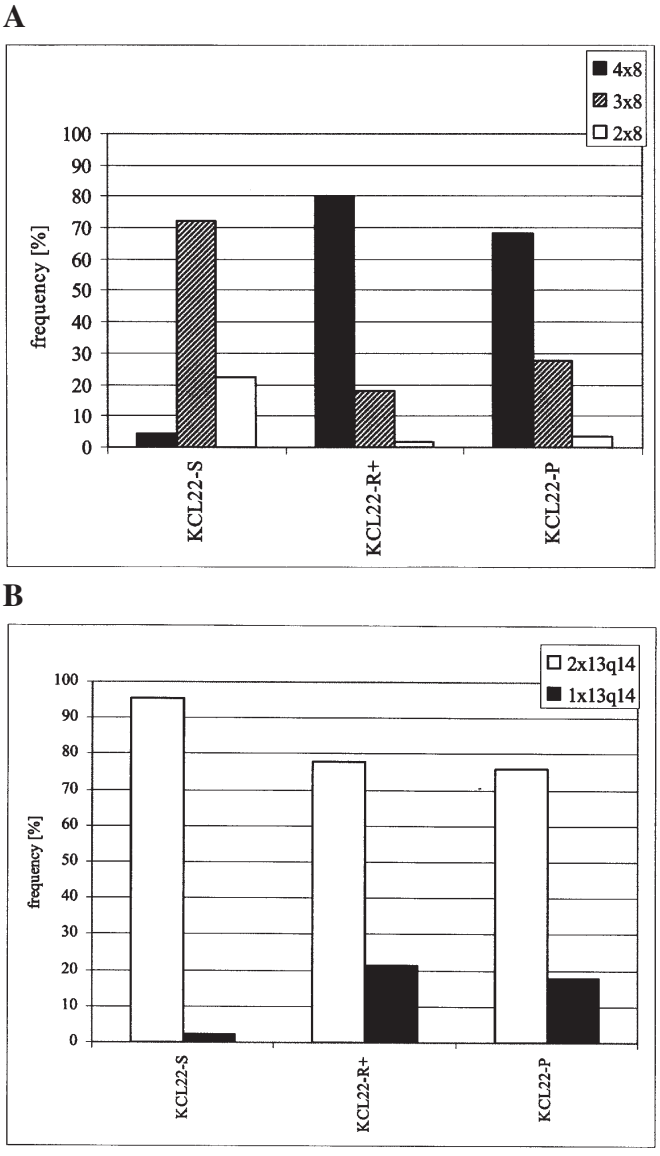

Figure 6. Subclones determined by interphase analysis with cep 8 (A) and LSI 13S319 (B). FISH probes in KCL22-S, continuously Imatinib-treated KCL22-R+ and the parental cell line KCL22-P.

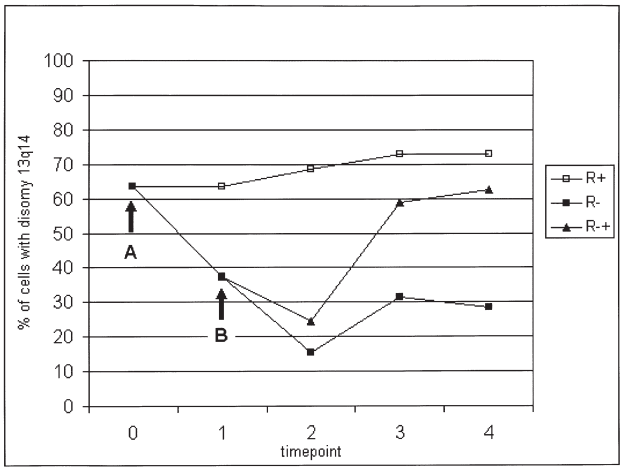

Figure 7. Modulation of the clone size of the sub-clones with a disomy 13q14 by Imatinib treatment versus those with a monosomy 13q14 by Interphase-FISH with LSI 13S319. □, data of continuously Imatinib-treated cells; ▲, data of Imatinib-deprived cells; ■, data of Imatinib re-treated cells. Arrow A marks the timepoint of withdrawal of Imatinib, B marks the time point of re-treatment with Imatinib.

questioned whether this could result from different growth properties of the different sub-clones in KCL22-R. Interestingly, withdrawal of Imatinib reduced the clone size of the cells with a disomy for 13q14 in favour of the monosomic cells from 64% to 16% within two weeks (KCL22-R-; Fig. 7). A proportion of the monosomic cells remained stable at approximately 21% in a follow-up of three months (Fig. 6). Vice versa, re-treatment of KCL22-R- with Imatinib restored the initial proportion of the disomic cells in favour of the monosomic cell population. The latter is shown in Fig. 7 by a deferred increase of disomic cell population to approximately 62% within 2-3 weeks.

ProteinChip (SELDI) profiling. Analysis of fractionated cell lysates revealed 45 differentially expressed proteins, 31 peaks were found overexpressed in the resistant cell line while 14 peaks were characteristic markers for the sensitive cell line (Table I). The majority of expression differences was found in the pH 9.0 fraction. For example, as shown in the cluster blot analysis (Fig. 8A) the peak with the molecular mass of 5468 Da showed an 8-fold overexpression in the sensitive cell line (median intensity, 129) compared to the resistant cell line (median intensity, 16) with a p value of 0.00071. The ROC curve analysis showed an area under curve (AUC) of 0.91. The 7482-Da peak was 6-fold overexpressed in the resistant cell line (median intensity 31 to 5, Fig. 8B) with an AUC of 0.89 and a p value of 0.00091. A representative SELDI spectra for these two peaks is depicted in Fig. 9.

Discussion

Cytogenetic and proteomic analysis of KCL22-R and KCL22-S has revealed common and discriminating aberrations between both cell lines. With cytogenetic analysis a tetrasomy 8 and a translocation t(6;13) are found to be characteristic for KCL22-R and absent in KCL22-S. These additional chromosomal anomalies in KCL22-R might result from the continuous exposure to Imatinib as the observed gain of chromosome anomalies in Imatinib-treated patients (13). The increment of chromosome aberrations is probably raised by the repressed wild-type ABL-kinase, an essential regulator of RAD51 that is known to promote DNA repair (30,31). The tetrasomy 8 was found in >80% of the KCL22-R cells but in <5% of KCL22-S (Fig. 6). Gain of chromosome 8 is one of the most frequent aberrations occurring in 34% in CML during disease progression (32). Among the numerous genes on chromosome 8 MAPKs, PTK2B, and the oncogene c-myc are the most prominent and potential players contributing to the BCR-ABL-independent growth control in KCL22-R. These putative candidates have not been analysed in the gene expression analysis of Tipping and co-workers (33). Therefore it remains open whether KCL22-R overexpresses these genes. However, since KCL22-S presented a trisomy-8, it seems unlikely that the tetrasomy-8 in KCL22-R will contribute significantly to the BCR-ABL-independent cell growth.

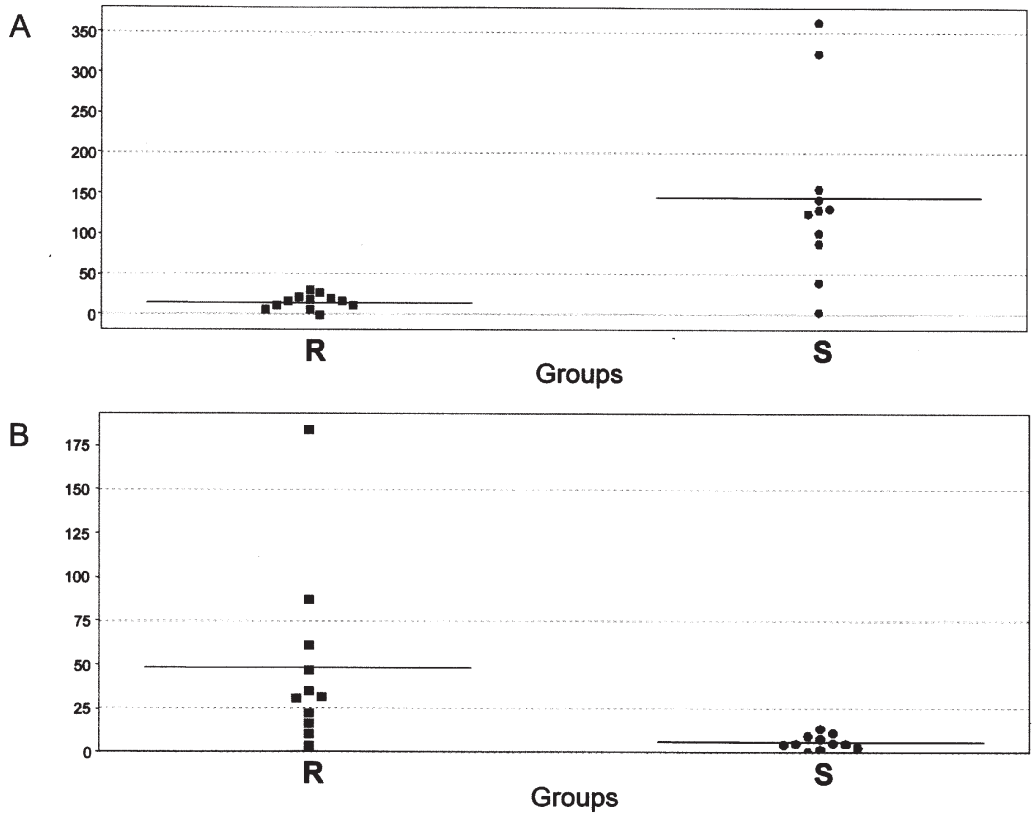

Figure 8. Cluster blot view of representative peaks analysed by protein profiling. The upper graph (A) shows a 12-fold overexpression of the 5468-Da peaks in the sensitive cell line, the lower graph (B) shows a 5.9-fold up-regulation of the 7482-Da peak in the resistant cell line.

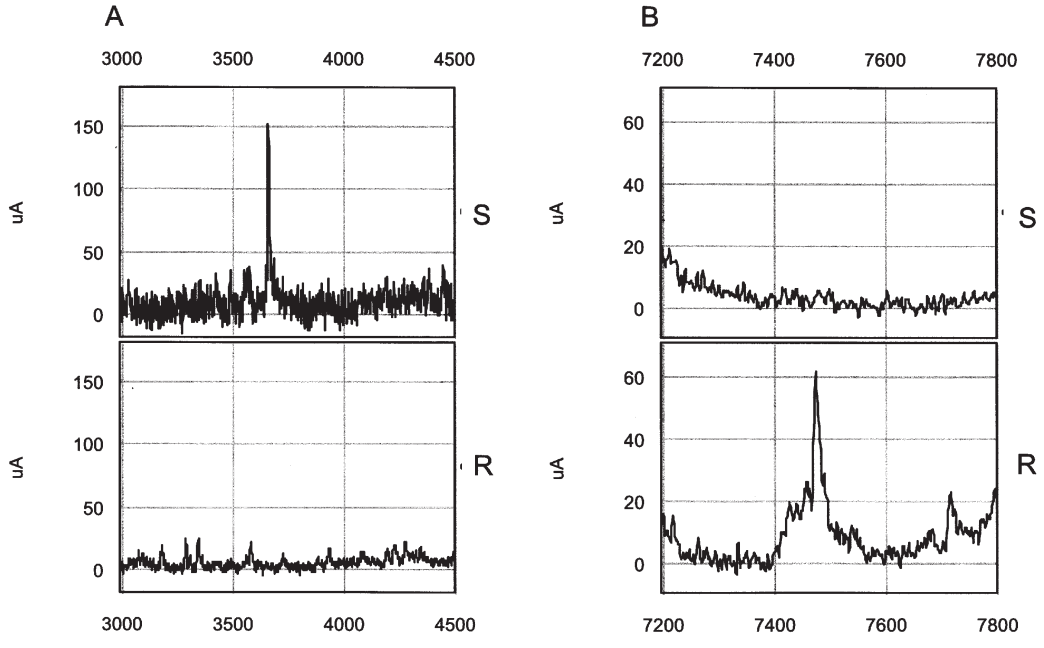

Figure 9. A representative SELDI spectra is depicted for the 5468-Da (A) and the 7482-Da peak (B).

The breakpoints of the second characteristic aberration of KCL22-R the translocation t(6;13), were mapped to (p11.1;p12) by multi-color banding. This aberration was not detected in KCL22-S nor in the parental cell line KCL22 which show an intermediate resistance against Imatinib compared to KCL22-R and KCL22-S (data not shown). This demands a more accurate mapping of the translocation breakpoint to detect potentially affected genes that contribute to the BCR-ABL-independent phenotype.

Noteworthily, chromosome der(6)t(6;13) showed a remarkable variability. This is documented by five variant clones with variable amounts of chromatin from 13q13 to

Table I. Differentially expressed protein peaks in KCL22-S and -R in fractionated samples.

Fraction	Molecular weight (Da)	p-value	AUC	Fold overexpression	S/R
F1 (pH 9.0)	3673	0.0017	0.88	7.40	S
	4225	0.005	0.87	2.80	R
	4559	0.002	0.89	3.90	R
	5444	0.003	0.85	7.20	S
	5468	0.0007	0.91	12.13	S
	5541	0.01	0.79	9.40	S
	6235	0.0004	0.72	3.00	R
	7482	0.0009	0.89	6.30	R
	9352	0.002	0.87	2.30	R
	9708	0.0007	0.9	4.50	R
	10380	0.0081	0.81	2.90	R
	11307	0.002	0.77	1.50	S
	11583	0.006	0.82	1.40	S
	25179	0.02	0.77	1.28	R
	25522	0.02	0.77	1.42	R
	54212	0.03	0.77	1.33	R
	67376	0.02	0.77	2.20	S
	78870	0.04	0.77	1.87	S
F2 (pH 7.0)	4088	0.002	0.94	5.20	R
	54214	0.0017	0.93	2.89	R
F3 (pH 5.0)	6061	0.002	0.87	8.70	S
	12260	0.03	0.77	3.60	R
	12438	0.02	0.77	2.18	R
	12507	0.0004	0.94	1.60	R
	13336	0.03	0.77	2.01	R
	17202	0.02	0.81	1.74	R
F4 (pH 4.0)	6074	0.007	0.82	5.60	S
	7964	0.002	0.9	3.60	R
	8617	0.008	0.81	1.70	R
	17432	0.002	0.81	1.50	R
	17921	0.047	0.71	1.59	R
	27251	0.013	0.77	1.50	S
	33167	0.035	0.8	1.52	R
	54324	0.047	0.74	1.40	R
	73867	0.013	0.75	5.50	R
	106852	0.03	0.81	1.80	S
F5 (pH 3.0)	7820	0.03	0.84	2.50	S
	11144	0.035	0.75	1.90	R
	11234	0.017	0.78	1.89	R
	11268	0.02	0.75	1.86	R
	11312	0.04	0.75	1.47	R
	15926	0.02	0.81	1.56	R
	19049	0.03	0.8	1.90	S
F6 (organic)	15065	0.02	0.82	2.02	R
	31728	0.045	0.72	1.50	R

13qter within the der(6)t(6;13) chromosome (Fig. 4). From the evolutionary point of view, this variation is expected to correlate with distinct growth properties. Effectively, Imatinib treatment was capable of modulating the clone size of the cells with different variants of the aberrant chromosome 6. In permanent Imatinib-treated KCL22-R (KCL22-R^{+}) we identified a disomy for 13q14 in the main cell population (65%). Interestingly, withdrawal of Imatinib reduced the number of 13q14 disomic cells in benefit of the 13q14 monosomic cells from 65% to 16% within two weeks as shown in Fig. 7 (KCL22-R^{-}). Thus the 13q14-qter disomic sub-clones have a growth disadvantage versus the 13q14-qter monosomic sub-clones in Imatinib-deprived KCL22-R. Re-treatment of KCL22-R^{-} with Imatinib restores the initial clone size of the disomic cells and reduces the monosomic cell population (KCL22-R^{-+}). It seems difficult to understand how the 13q14 monosomic, Imatinib-sensitive clone has evolved and is preserved in permanently Imatinib-treated KCL22-R. However, it is conceivable that loss of Imatinib stability before the next cell passage may give this clone sufficient time to 'catch up'. This explanation is supported by the rapid and dramatic clone expansion that we observed in Imatinib-deprived and retreated KCL22-R.

We have shown that Imatinib has a positive effect on cell growth of KCL22-R. From this we conclude that active BCR-ABL or other Imatinib-sensitive kinases act negatively on cell proliferation. The data described above indicate that this effect is restricted to some KCL22-R sub-clones. This also explains the attenuated cell growth and increased apoptosis rate of KCL22-R after Imatinib withdrawal. Similar results were reported for the cell lines BaF/BCR-ABL and LAMA84 where withdrawal of Imatinib induced apoptosis (34).

Active BCR-ABL could induce apoptosis via JNK/SAPK after activation through Ras (35,36). It can be assumed that it also inhibits cell proliferation via the Rb gene as is observed for ABL (37). Rb is localized in 13q14.3 and is therefore lost in the truncated der(6)t(6;13) that marks the predominant sub-clone of Imatinib-deprived KCL22-R cells. However, we have no evidence so far that loss of heterozygosity of Rb is causal for the distinct growth behaviour of the KCL22-R^{-} subclones.

There are many other genes in 13q14_qter that could contribute to this different growth behaviour of the 13q14 disomic and monosomic sub-clones in KCL22-R. Considering the fact that Imatinib acts anti-apoptotically and promotes cell growth of BCR-ABL-independent CML clones, clinical application of Imatinib should be critically reconsidered in advanced disease stages.

The proteomic analysis of the two cell lines performed with ProteinChip Arrays revealed several differentially expressed proteins that could be linked to the described chromosomal changes. Forty-five proteins were found with significantly changed intensities in KCL22-S and -R. These proteins must be identified and could probably be assigned to the altered chromosomal regions described above. Whether these proteins can be linked to signal transduction pathways that play a role in the BCR-ABL-independent growth of CML cells will be investigated further. This may reveal new targets for therapy of primary Imatinib-resistant CML patients.

Acknowledgements

We would like to thank Junia Melo for providing the KCL22-S and -R cell lines, Andrea Uecker for supplying Imatinib and especially Klaus Weisshart and Ryan Oyama for critically proof-reading our manuscript. This study was supported by a grant from the German Federal Ministry of Education and Research (BMBF) and the Interdisciplinary Center for Clinical Research (ICCR), Jena.

Reference

1. Rowley JD: Letter: A new consistent chromosomal abnormality in chronic myelogenous leukaemia identified by quinacrine fluorescence and Giemsa staining. Nature 243: 290-293, 1973.
2. Bartram CR, de Klein A, Hagemeijer A, van Agthoven T, Geurts VK, Bootsma D, Grosveld G, Ferguson-Smith MA, Davies T and Stone M: Translocation of c-ab1 oncogene correlates with the presence of a Philadelphia chromosome in chronic myelocytic leukaemia. Nature 306: 277-280, 1983.
3. Lugo TG, Pendergast AM, Muller AJ and Witte ON: Tyrosine kinase activity and transformation potency of bcr-abl oncogene products. Science 247: 1079-1082, 1990.
4. Deininger MWN, Goldman JM and Melo JV: The molecular biology of chronic myeloid leukemia. Blood 96: 3343-3356, 2000.
5. Melo JV, Hughes TP and Apperley JF: Chronic Myeloid Leukemia. Hematology: 132-152, 2003.
6. Deininger M, Buchdunger E and Druker BJ: The development of imatinib as a therapeutic agent for chronic myeloid leukemia. Blood 105: 2640-2653, 2005.
7. Gorre ME, Mohammed M, Ellwood K, Hsu N, Paquette R, Rao PN and Sawyers CL: Clinical resistance to STI-571 cancer therapy caused by BCR-ABL gene mutation or amplification. Science 293: 876-880, 2001.
8. Barthe C, Gharbi Mj, Lagarde V, Chollet C, Cony-Makhoul P, Reiffers J, Goldman JM, Melo JV and Mahon FX: Mutation in the ATP-binding site of BCR-ABL in a patient with chronic myeloid leukaemia with increasing resistance to STI571. Br J Haematol 119: 109-111, 2002.
9. Gambacorti-Passerini C, Gundry R, Piazza R, Galietta A, Rostagno R and Scapozza L: Molecular mechanisms of resistance to imatinib in Philadelphia-chromosome-positive leukaemias. Lancet Oncol 4: 75-85, 2003.
10. Hochhaus A: Cytogenetic and molecular mechanisms of resistance to imatinib. Semin Hematol 40: 69-79, 2003.
11. Cortes J and O'Dwyer ME: Clonal evolution in chronic myelogenous leukemia. Hematol Oncol Clin North Am 18: 671-684, 2004.
12. Bacher U, Haferlach T, Hiddemann W, Schnittger S, Kern W and Schoch C: Additional clonal abnormalities in Philadelphia-positive ALL and CML demonstrate a different cytogenetic pattern at diagnosis and follow different pathways at progression. Cancer Genet Cytogenet 157: 53-61, 2005.
13. Fabarius A, Giehl M, Frank O, Duesberg P, Hochhaus A, Hehlmann R and Seifarth W: Induction of centrosome and chromosome aberrations by imatinib *in vitro*. Leukemia 19: 1573-1578, 2005.
14. Tang N, Tornatore P and Weinberger SR: Current developments in SELDI affinity technology. Mass Spectrom Rev 23: 34-44, 2004.
15. Paradis V, Degos F, Dargere D, Pham N, Belghiti J, Degott C, Janeau JL, Bezeaud A, Delforge D, Cubizolles M, Laurendeau I and Bedossa P: Identification of a new marker of hepatocellular carcinoma by serum protein profiling of patients with chronic liver diseases. Hepatology 41: 40-47, 2005.
16. Li Y, Dang TA, Shen J, Perlaky L, Hicks J, Murray J, Meyer W, Chintagumpala M, Lau CC and Man TK: Identification of a plasma proteomic signature to distinguish pediatric osteosarcoma from benign osteochondroma. Proteomics 6: 3426-3435, 2006.
17. Bali P, Pranpat M, Bradner J, Balasis M, Fiskus W, Guo F, Rocha K, Kumaraswamy S, Boyapalle S, Atadja P, Seto E and Bhalla K: Inhibition of histone deacetylase 6 acetylates and disrupts the chaperone function of heat shock protein 90: A novel basis for antileukemia activity of histone deacetylase inhibitors. J Biol Chem 280: 26729-26734, 2005.
18. Melle C, Ernst G, Schimmel B, Bleul A, Mothes H, Kaufmann R, Settmacher U and von Eggeling F: Different expression of calgizzarin (S100A11) in normal colonic epithelium, adenoma and colorectal carcinoma. Int J Oncol 28: 195-200, 2006.
19. Cheung PK, Woolcock B, Adomat H, Sutcliffe M, Bainbridge TC, Jones EC, Webber D, Kinahan T, Sadar M, Gleave ME and Vielkind J: Protein profiling of microdissected prostate tissue links growth differentiation factor 15 to prostate carcinogenesis. Cancer Res 64: 5929-5933, 2004.
20. Melle C, Kaufmann R, Hommann M, Bleul A, Driesch D, Ernst G and von Eggeling F: Proteomic profiling in microdissected hepatocellular carcinoma tissue using ProteinChip technology. Int J Oncol 24: 885-891, 2004.
21. Melle C, Bogumil R, Ernst G, Schimmel B, Bleul A and von Eggeling F: Detection and identification of heat shock protein 10 as a biomarker in colorectal cancer by protein profiling. Proteomics 6: 2600-2608, 2006.
22. Escher N, Spies-Weisshart B, Kaatz M, Melle C, Bleul A, Driesch D, Wollina U and von Eggeling F: Identification of HNP3 as a tumour marker in $CD4^+$ and $CD4^-$ lymphocytes of patients with cutaneous T-cell lymphoma. Eur J Cancer 42: 249-255, 2006.
23. Mahon FX, Deininger MWN, Schultheis B, Chabrol J, Reiffers J, Goldman JM and Melo JV: Selection and characterization of BCR-ABL positive cell lines with differential sensitivity to the tyrosine kinase inhibitor STI571: diverse mechanisms of resistance. Blood 96: 1070-1079, 2000.
24. Verma R and Babu A: Human Chromosomes. Elsevier Science Ltd, 1989.
25. Weise A, Liehr T, Efferth T, Kuechler A and Gebhart E: Comparative M-FISH and CGH analyses in sensitive and drug-resistant human T-cell acute leukemia cell lines. Cytogenet Genome Res 98: 118-125, 2002.
26. Stentoft J, Pallisgaard N, Kjeldsen E, Holm MS, Nielsen JL and Hokland P: Kinetics of BCR-ABL fusion transcript levels in chronic myeloid leukemia patients treated with STI571 measured by quantitative real-time polymerase chain reaction. Eur J Haematol 67: 302-308, 2001.
27. Liehr T, Heller A, Starke H, Rubtsov N, Trifonov V, Mrasek K, Weise A, Kuechler A and Claussen U: Microdissection based high resolution multicolor banding for all 24 human chromosomes. Int J Mol Med 9: 335-339, 2002.
28. Kriegova E, Melle C, Kolek V, Hutyrova B, Mrazek F, Bleul A, du Bois RM, von Eggeling F and Petrek M: Protein profiles of bronchoalveolar lavage fluid from patients with pulmonary sarcoidosis. Am J Respir Crit Care Med 173: 1145-1154, 2006.
29. Kubonishi I and Miyoshi I: Establishment of a Ph1 chromosome-positive cell line from chronic myelogenous leukemia in blast crisis. Int J Cell Cloning 1: 105-117, 1983.
30. Yuan ZM, Huang Y, Ishiko T, Nakada S, Utsugisawa T, Kharbanda S, Wang R, Sung P, Shinohara A, Weichselbaum R and Kufe D: Regulation of Rad51 function by c-Abl in response to DNA damage. J Biol Chem 273: 3799-3802, 1998.
31. Russell JS, Brady K, Burgan WE, Cerra MA, Oswald KA, Camphausen K and Tofilon PJ: Gleevec-mediated inhibition of Rad51 expression and enhancement of tumor cell radiosensitivity. Cancer Res 63: 7377-7383, 2003.
32. Johansson B, Fioretos T and Mitelman F: Cytogenetic and molecular genetic evolution of chronic myeloid leukemia. Acta Haematol 107: 76-94, 2002.
33. Tipping AJ, Deininger MW, Goldman JM and Melo JV: Comparative gene expression profile of chronic myeloid leukemia cells innately resistant to imatinib mesylate. Exp Hematol 31: 1073-1080, 2003.
34. Desplat V, Belloc F, Lagarde V, Boyer C, Melo JV, Reiffers J, Praloran V and Mahon FX: Overproduction of BCR-ABL induces apoptosis in imatinib mesylate-resistant cell lines. Cancer 103: 102-110, 2005.
35. Raitano AB, Halpern JR, Hambuch TM and Sawyers CL: The Bcr-Abl leukemia oncogene activates Jun kinase and requires Jun for transformation. PNAS 92: 11746-11750, 1995.
36. Ho FM, Liu SH, Liau CS, Huang PJ and Lin-Shiau SY: High glucose-induced apoptosis in human endothelial cells is mediated by sequential activations of c-Jun NH2-terminal kinase and caspase-3. Circulation 101: 2618-2624, 2000.
37. Trimarchi JM and Lees JA: Sibling rivalry in the E2F family. Nat Rev Mol Cell Biol 3: 11-20, 2002.